AGU PUBLICATIONS

JGR

Journal of Geophysical Research: Space Physics

RESEARCH ARTICLE
10.1002/2017JA024249

Key Points:
- Three types of relativistic electron precipitation are confirmed on the basis of more than thousand events detected by POES satellites
- A quarter of REP events conjugated with ground magnetometers is connected with the source of geomagnetic pulsations in the EMIC wave range
- This poses the question on whether EMIC waves play a main role in the precipitation of electrons with energy of approximately 1 MeV

Correspondence to:
A. G. Yahnin,
yahnin@pgia.ru

Citation:
Yahnin, A. G., T. A. Yahnina, T. Raita, and J. Manninen (2017), Ground pulsation magnetometer observations conjugated with relativistic electron precipitation, *J. Geophys. Res. Space Physics*, *122*, 9169–9182, doi:10.1002/2017JA024249.

Received 11 APR 2017
Accepted 1 AUG 2017
Accepted article online 14 AUG 2017
Published online 2 SEP 2017

Ground pulsation magnetometer observations conjugated with relativistic electron precipitation

A. G. Yahnin[1], T. A. Yahnina[1], T. Raita[2], and J. Manninen[2]

[1]Polar Geophysical Institute, Apatity, Russia, [2]Sodankylä Geophysical Observatory, University of Oulu, Sodankylä, Finland

Abstract In this report, we investigate the role of electromagnetic ion cyclotron (EMIC) waves in production of relativistic electron precipitation (REP). Over a thousand REP events were detected from four NOAA Polar-orbiting Operational Environmental Satellites in July–December 2005. Of these, a total of 112 events were conjugated with a ground-based network of six Finnish induction coil magnetometers and one in Lovozero observatory at Kola Peninsula, Russia. The observation of geomagnetic pulsations during the conjugated events showed that about one third of them were accompanied by pulsations in the Pc1 range, which are the signature of EMIC waves. In fact, the sources of some of these EMIC waves were well outside the location of the REP event. This means that in such cases the REP events were not originated from scattering by EMIC waves. Finally, it is concluded that for this limited set of conjugated events only a quarter might be related to scattering by EMIC waves. The majority of the events are not correlated with EMIC wave signatures in ground-based observations; they were associated with either no pulsations or noise-like pulsations PiB and PiC.

1. Introduction

Different mechanisms are able to produce the precipitation of relativistic electrons from the outer radiation belt. Such electrons can be scattered into the loss cone by different waves, for example, by electromagnetic ion cyclotron (EMIC) waves, hiss and chorus waves [e.g., *Summers et al*., 2007], and upper hybrid resonance (UHR) waves [*Shklyar and Kliem*, 2006]. Scattering of charged particles from the equatorial region where the magnetic field line curvature is relatively small [e.g., *Sergeev and Tsyganenko*, 1982] has also been proved as possible mechanism for the relativistic electron precipitation (REP) [e.g., *Imhof et al*., 1991; *Yahnin et al*., 2016; *Smith et al*., 2016].

Interaction with EMIC waves is often believed to be the most important mechanism for relativistic electron scattering because these waves provide the highest pitch angle diffusion rate for >1 MeV electrons near the loss cone in comparison with other waves [e.g., *Summers et al*., 2007]. This mechanism is expected to operate mainly in the afternoon and at the dusk where the conditions for ion cyclotron instability are predicted to be favorable [e.g., *Thorne and Kennel*, 1971; *Chen et al*., 2009]. Magnetospheric observations point out the maximal occurrence of the EMIC waves in the afternoon-dusk sector [*Anderson et al*., 1992; *Halford et al*., 2010; *Usanova et al*., 2012; *Keika et al*., 2013]. Recent studies have aimed to confirm the EMIC wave mechanism of the REP. Some of them were based on the indirect indications of the EMIC wave presence. For example, *Sandanger et al*. [2007], *Miyoshi et al*. [2008], and *Carson et al*. [2013] used the simultaneous observations of energetic proton precipitation spikes. Some studies were focused on the conjugated REP and EMIC wave observations [*Rodger et al*., 2015; *Blum et al*., 2015; *Hendry et al*., 2016]. *Blum et al*. [2013, 2015] considered a case of a strong REP event related with EMIC waves and concluded that such events could significantly deplete the outer radiation belt.

At the same time, it is not evident how common is the scattering by EMIC waves in comparison with other possible REP mechanisms. In the recent paper by *Yahnin et al*. [2016] the proportions between different mechanisms producing REP events were established on the basis of observations on board NOAA Polar-orbiting Operational Environmental Satellites (POES). This was made using combined proton and electron precipitation in different energy ranges. As a signature of EMIC waves, the localized precipitation of energetic (tens of keV) protons equatorward of the proton isotropy boundary was assumed [e.g., *Yahnina et al*., 2003; *Yahnin et al*., 2007, 2009; *Yahnin and Yahnina*, 2007; *Sakaguchi et al*., 2007; *Morley et al*., 2009]. Coincidence of the proton and relativistic electron precipitation was, therefore, considered as a signature of the "EMIC wave-driven" REP [*Miyoshi et al*., 2008; *Sandanger et al*., 2007; *Carson et al*., 2013; *Hendry et al*., 2016]. According to

Yahnin et al. [2016], interaction with EMIC waves could produce relatively small fraction of all REP events (17%). It is worth to note that this conclusion was based on indirect evidence because no wave observations were involved.

This report is aimed at checking this conclusion with the addition of the wave measurements. As is well known, EMIC waves generated in the equatorial magnetosphere have signatures on the ground in form of geomagnetic pulsations in the frequency range from 0.1 to a few hertz [e.g., *Kangas et al*., 1998]. They are Pc1 and Pc2 pulsations, intervals of pulsations of diminishing periods (IPDP), and bursts of pulsations in the above frequency range (Pc1 bursts). The Pc1-Pc2 pulsations are continuous quasi-monochromatic emissions with the midfrequency exhibiting only small and slow variations [e.g., *Fukunishi et al*., 1981; *Kangas et al*., 1998]. These pulsations typically occur during recovery phase of magnetic storms. The IPDP resemble Pc1, whose frequency significantly increases in time (typically from 0.2 to 1–2 Hz). They have duration of ~1 h, and they often relate to development of substorms [e.g., *Troitskaya*, 1961; *Pikkarainen et al*., 1983; *Hayakawa et al*., 1992]. Pc1 bursts have duration of few minutes and occur during magnetosphere compressions [*Anderson and Hamilton*, 1993; *Anderson et al*., 1996; *Zhang et al*., 2008; *Yahnina et al*., 2008].

We will consider how the REP events measured on board NOAA POES satellites correlate with observations of these EMIC wave signatures. The next section describes the data, selection of the REP events and their classification. In section 3, some spectrograms of geomagnetic pulsations in the Pc1 range during REP events are presented, and the relationship between different types of REP and geomagnetic pulsations is investigated. The Discussion and Conclusions will be given in sections 4 and 5, respectively.

2. Data, REP Selection, and Classification

2.1. POES Data

The data from four NOAA POES spacecraft (NOAA 15, 16, 17, and 18) for the 6 month interval from 1 July to 31 December 2005 are used in this study. The spacecraft was flying at circular polar orbits at altitude ~800 km. Each spacecraft is equipped with identical Medium Energetic Proton and Electron Detector (MEPED) instrument, which has, in particular, two (electron and proton) pairs of directional telescopes [*Evans and Greer*, 2004]. In each pair, one telescope is directed to zenith and another one "looks" against the direction of travel (0° and 90° telescopes, respectively). In the region of interest ($L > 3$) the 0° telescopes measure precipitating particles (within the loss cone), while the 90° telescopes measure predominantly trapped particles [e.g., *Rodger et al*., 2010a, 2010b]. The electron directional telescopes have three integral channels E1, E2, and E3 (nominal low-cutoff energies are 30, 100, and 300 keV, respectively). The proton directional telescopes measure ions in six energy channels: P1 (30–80 keV), P2 (80–250 keV), P3 (250–800 keV), P4 (800–2500 keV), P5 (2500–6900 keV), and P6 (>6900 keV).

The electron and most of proton channels are subject to the contamination by protons and electrons, respectively [*Yando et al*., 2011; *Evans and Greer*, 2004]. For our study, it is important that the P6 channel is contaminated by relativistic (>800 keV) electrons while the P5 channel is not sensitive to electrons. The >800 keV electrons produce the response in the P6 channel comparable to the >6.9 MeV protons of the same flux [*Yando et al*., 2011]. Thus, the P6 channel can measure >6.9 MeV protons or relativistic electrons or both. We identified the enhancements in the 0° telescope of the P6 channel as REP if they were associated with the lack of signal in the P5 channel.

For further REP event selection, we used the same criteria as *Yahnin et al*. [2016]: The enhancements of precipitating relativistic electrons with intensity below 5 c/s and duration shorter than 4 s were not taken into account. The latter criterion means that we select so-called precipitation band events [e.g., *Nakamura et al*., 1995] but not possibly chorus-related microbursts, which have duration shorter than 1 s. The NOAA POES passes in the vicinity of the South Atlantic Magnetic Anomaly were excluded from the consideration, as done by *Carson et al*. [2013, see their Figure 2]. The selected REP events were analyzed along with other data from the MEPED electron and proton telescopes. Total amount of 1057 REP events were detected on board POES satellites during the studied 6 month interval.

2.2. Geomagnetic Conditions

The interval under study is characterized by variable geomagnetic activity including three strong magnetic storms in the end of August and during September 2005 (Figures 1a–1c). The mean values of geomagnetic

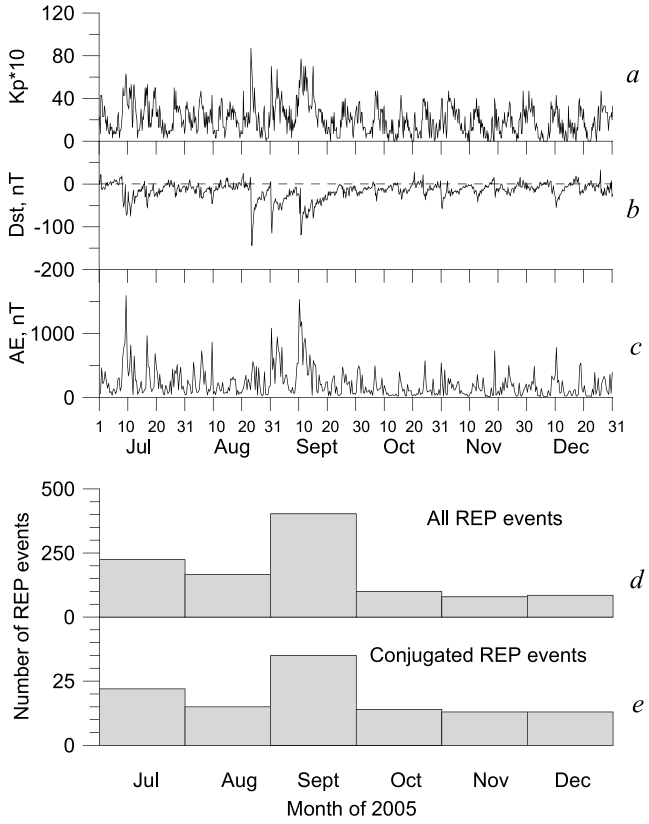

Figure 1. (a–c) Indices of geomagnetic activity *Kp*×10, *Dst*, *AE* for the interval from 1 July to 31 December 2005. (d) Monthly number of REP events for the interval under study. (e) Monthly number of REP events conjugated with ground network of induction magnetometers.

activity indices *AE*, *Kp*×10, and *Dst* for the whole interval were 213 nT, 21, and −16 nT, respectively. Interestingly, the values of these indices during the REP events were 411 nT, 32, −28 nT, respectively. This means that REP events tend to occur during periods of the enhanced activity. For example, the number of REP events was maximal during September 2005 (403 events under monthly mean *AE* index equal to 302 nT) and minimal during October–December (about 90 events per month under monthly mean *AE* index equal to 153 nT) (Figure 1d).

2.3. Ground Pulsation Magnetometer Network

For this study, we used the data from the Finnish network of induction coil magnetometers operated by Sodankylä Geophysical Observatory and magnetometer in observatory Lovozero at Kola Peninsula operated by Polar Geophysical Institute in Apatity/Murmansk, Russia. Locations of the stations in geographic and Corrected GeoMagnetic (CGM) coordinates are listed in Table 1 and plotted in Figure 2. (The CGM coordinates are calculated by tracing the given geographic location to the magnetic equator using International Geomagnetic Reference Field model, and then tracing it back using the dipole magnetic field [e.g., *Gustafsson et al*., 1992, and references therein]). The induction coil magnetometers have the sampling rate 40 sample/s. The spectrograms of geomagnetic pulsations in the range of 0.1–5 Hz are used to identify the ground-based wave activity and total power density spectrums for details of selected events.

Besides pulsations representing EMIC waves (quasi-monochromatic Pc1-Pc2 emissions, IPDP, Pc1 bursts), some other kinds of pulsations can be seen on the spectrograms. They are the following: (1) PiB, that is, the short (~1 min) bursts of low frequency (up to ~1 Hz) noise indicating substorm onsets and substorm activations [e.g., *Heacock*, 1967; *Bösinger and Yahnin*, 1987] and (2) PiC, continuous irregular emissions in the range up to few tens of hertz, typically occurring during negative magnetic bays [e.g., *Heacock*, 1967]. Sometimes, unclassified low-frequency noise intensifications are observed, which is, probably, a subclass of PiC pulsations.

Table 1. List of Ground-Based Stations and Their Locations

		Geographic		CGM[a]	
Station Name	Abbreviation	Latitude	Longitude	Latitude	Longitude
Kilpisjarvi	KIL	69.02°N	20.86°E	65.96	103.75
Ivalo	IVA	68.55°N	27.28°E	65.18	108.51
Sodankyla	SOD	67.42°N	26.39°E	64.07	107.05
Rovaniemi	ROV	66.78°N	25.94°E	63.43	106.30
Oulu	OUL	65.08°N	25.90°E	61.69	105.31
Nurmijarvi	NUR	60.51°N	24.65°E	56.98	102.18
Lovozero	LOZ	68.01°N	35.03°E	64.36	114.50

[a]The corrected geomagnetic coordinates are calculated for epoch 2005 and altitude 110 km.

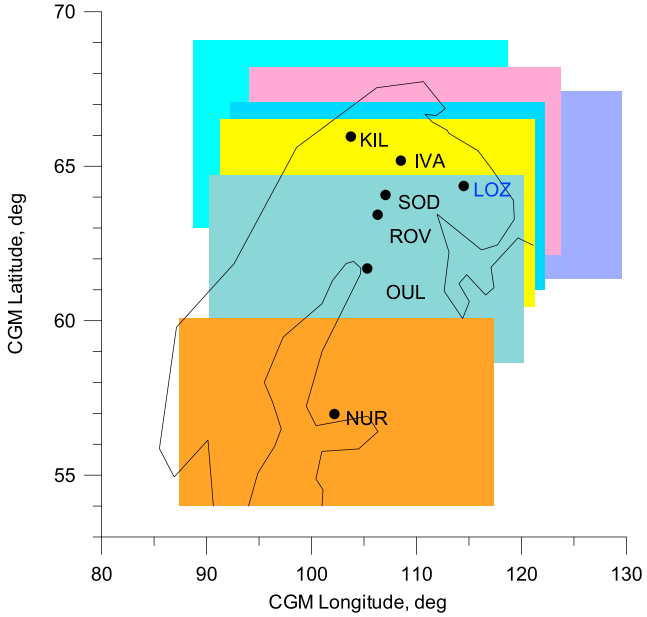

Figure 2. Map of ground-based induction magnetometers in Finland and at Kola Peninsula used in this study in corrected geomagnetic coordinates. Colored rectangles show areas around each station, which are bounded with ±3° of latitude and ±15° of longitude.

2.4. Classification of REP Events

The events were divided into three groups according to the interrelation between REP (enhancements of precipitating >0.8 MeV electrons measured in the P6 channel) and fluxes in other electron and proton channels [see *Yahnin et al.*, 2016, their section 3.1, Figure 2, and Table 1]. It has been suggested [e.g., *Imhof et al.*, 1986, 1991; *Yahnin et al.*, 2016] that REP events of different groups are probably produced by different mechanisms.

According to *Yahnin et al.* [2016], the REP events of the *first* group coincide with transition between isotropic and anisotropic fluxes (isotropy boundary) of relativistic (>0.8 MeV) electrons. These events do not coincide with any enhancements of precipitating electrons of lower energies measured in channels E1–E3 as well as with any precipitating proton enhancements. The isotropy boundaries of electrons measured in channels E1–E3 are poleward, while the isotropy boundaries of >30 keV protons are equatorward of the REP location. Such latitudinal dependence of the isotropy boundary location is consistent with the mechanism of scattering of charged particles in the regions where the movement of particles becomes nonadiabatic when the gyroradius of a particle is comparable with the curvature radius of the magnetic field line [e.g., *Sergeev and Tsyganenko*, 1982]. The particles having smaller gyroradius will be scattered at larger distances, and the boundary of the isotropic fluxes will be mapped on higher latitudes. The importance of this mechanism for the precipitation of relativistic electrons has been stressed, for example, by *Imhof et al.* [1991], *Nakamura et al.* [2000], and *Smith et al.* [2016]. The REP events of the *second* group occur equatorward of the isotropy boundary of >0.8 MeV electrons, inside the radiation belt. They occur simultaneously with the precipitation of electrons measured in the E1–E3 channels. Such REP events are not associated with any precipitating proton enhancements and can be observed on both sides of the proton isotropy boundary. The possible mechanism of these REP events relates to scattering by waves (probably, by hiss or UHR waves) (see discussion in *Yahnin et al.* [2016]). Finally, the REP events of the *third* group coincide with the enhancements in precipitating >30 keV protons (and almost always with the simultaneous enhancements of energetic electrons). Therefore, they can be considered as the "EMIC wave-driven" REP [*Carson et al.*, 2013]. Such REP events occur equatorward of the proton isotropy boundary and, correspondingly, well equatorward of the isotropy boundary of >0.8 MeV electrons, inside the radiation belt. It is worth to note that the REP events, which we associate with the *second* and *third* groups, have been studied by *Imhof et al.* [1986], who concluded that these events could be related to scattering by some low-frequency waves.

Within the studied interval we found 276, 621, and 160 events of the *first*, *second*, and *third* groups, respectively. Figure 3 (top row) shows Magnetic Local Time/CGM latitude (MLT/CGMLat) distributions of REP events for the whole data set. These distributions are very similar to those obtained by *Yahnin et al.* [2016] (see their Figure 4). The events of the *first* group are observed in the night sector. The events of the *second* group can be found at almost all MLTs, but the maximal amount is in the premidnight and night sector. The events of the *third* group are in the afternoon-premidnight sector.

2.5. Conjugated Events

We will consider those precipitation events, which are conjugated with ground stations measuring geomagnetic pulsations. As a criterion for the conjunction, we use the location of the REP event within ±15° of CGM

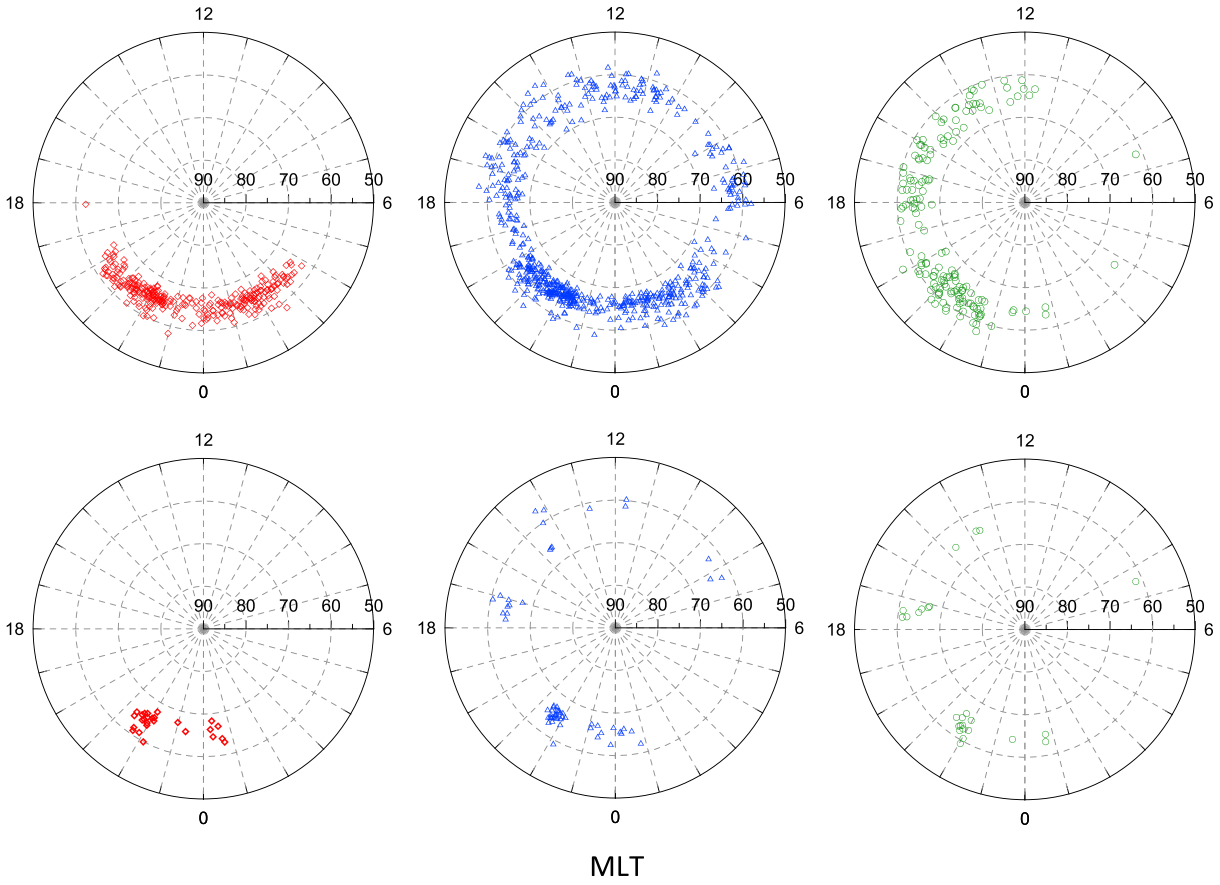

Figure 3. (top row) Distribution of the REP events of the first, second, and third group (red, blue, and green symbols, respectively) in MLT-CGMLat coordinates for time interval from 1 July to 31 December 2005. (bottom row) The same but for events conjugated with ground network of induction magnetometers.

longitude (±1 h of MLT) and ±3° in CGM latitude relatively to one of the ground stations. *Hendry et al.* [2016] used similar criteria except they used $\Delta L < 1$ instead of ΔCGMLat $< 3°$. These authors demonstrated high probability to observe the pulsations in the Pc1-Pc2 range during the "EMIC wave-driven" REP observations within these limits relatively to a ground station. Rectangles in Figure 2 show the area of conjunction for each ground station. The result of the search was 112 conjugated events (23 events in the *first* group, 63 events in the *second* group, and 26 events in the *third* group). The distribution of conjugated events in the MLT/CGMLat coordinates is shown in Figure 3 (bottom row).

Figure 4 presents a superposed epoch analysis of a latitudinal behavior of the particle fluxes relatively to the position of the REP event maximum for each group of conjugated events and for each electron and proton channel. Besides traces of the particle flux intensity for each POES pass (thin lines), the median values of trapped and precipitating flux (thick lines) are shown. It is clearly seen that main features of different kinds of the REP events are well reproduced in this plot (compare to Figure 1 and Table 1 by *Yahnin et al.* [2016] and to the above description of the three REP groups). The REP of the *first* group is at the outer edge of the trapped particles and is located equatorward of isotropy boundaries of lower energy electrons and poleward of the isotropy boundaries of protons (Figure 4a); the REP of the *second* group coincided with the spikes of subrelativistic electrons but not protons (Figure 4b); the REP of the *third* group coincides with enhancement in the proton flux as well as in the flux of subrelativistic electrons (Figure 4c). Thus, the conjugated events are suitable representatives of their groups, although their amount is significantly less than that in the whole data set.

Representativity of the conjugated events is also confirmed by their relation to geomagnetic activity. These events also occur under enhanced magnetic activity ($<AE> = 344$ nT, $<Kp\times10> = 29$, $<Dst> = -26$) in comparison with that averaged for the whole interval (see section 2.2). Also, the variation of the monthly number of the events is well correlated with that for the whole data set (Figure 1e).

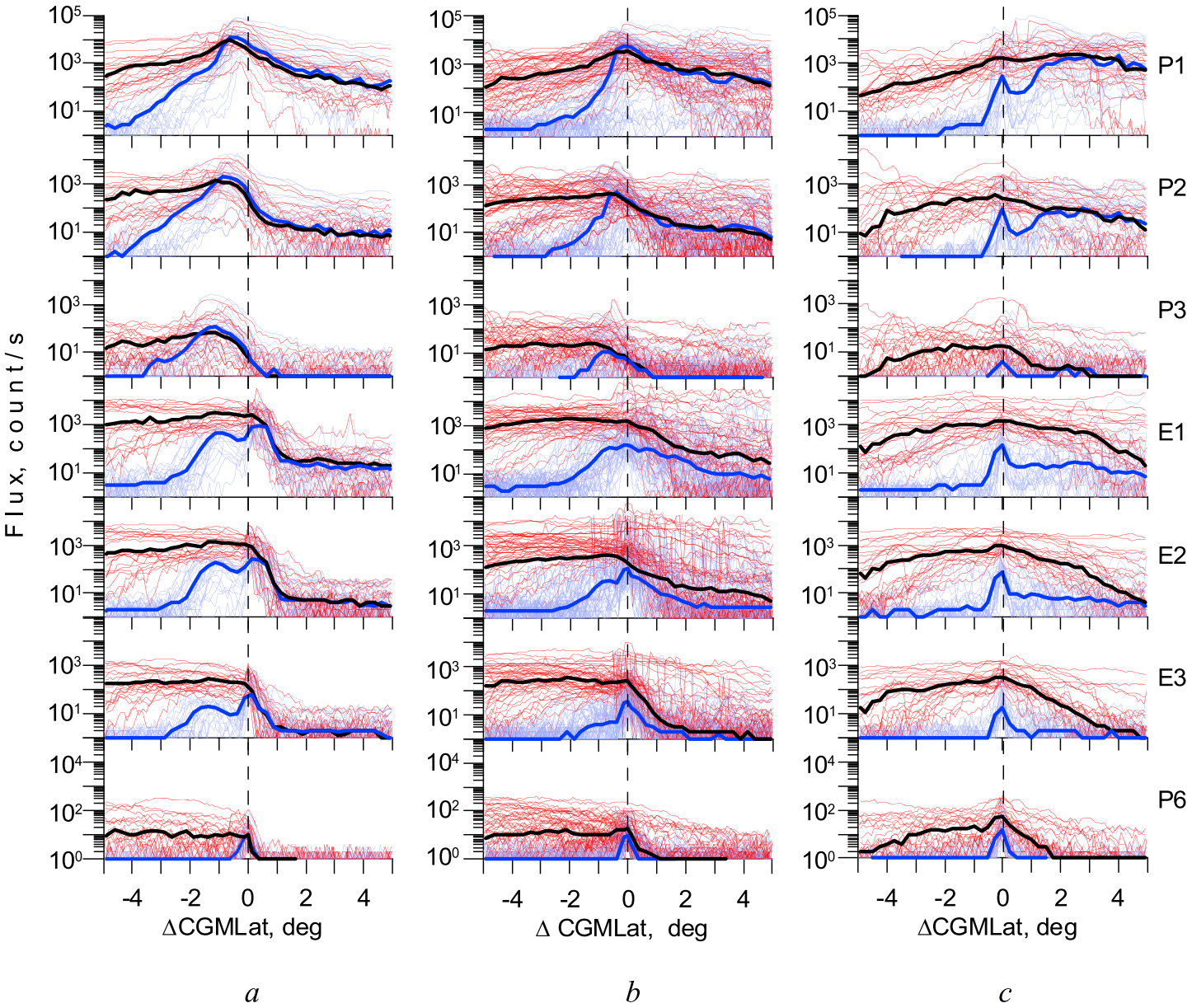

Figure 4. (a–c) Superposed epoch analysis of latitudinal variations of the particle fluxes in channels P1–P3, E1–E3, and P6 of the MEPED instrument for all conjugated events of the *first*, *second*, and *third* group of REP events, respectively. The latitude of maximum of the precipitating electron flux in the channel P6 (REP) marked by the vertical dashed line is used as the reference latitude. Positive (negative) values of ΔCGMLat (the satellite latitude relatively to the reference one) mean higher (lower) latitudes relatively to the position of the REP maximum. From top to bottom: The data from the channel P1 (protons, Ep = 30–80 keV), P2 (protons, Ep = 80–250 keV), and P3 (protons, 250–800 keV), E1 (electrons, $Ee > 30$ keV), E2 (electrons, $Ee > 100$ keV), E3 (electrons, $Ee > 300$ keV), P6 (electrons, $Ee > 800$ keV) are shown. The precipitating (trapped) fluxes are shown by the thin blue (red) lines. The median values of the precipitating (trapped) fluxes are shown by thick blue (black) lines.

3. Results of the REP and Pulsation Comparison

Inspection of the spectrograms of ground stations revealed 37 cases of 112 conjugated REP events where the REP event was observed simultaneously with Pc1, IPDP, and Pc1 bursts (that is, EMIC wave signatures). This is about a third of all REP events. Let us check how the REP events of different groups separately correlate with EMIC wave signatures.

Figures 5a and 5b show two REP events of the *first* group conjugated with ground observatories. The corresponding spectrograms are shown in Figures 5c and 5d. Enhancement of low-frequency magnetic noise was observed during the REP event of 17 September 2005. The REP event of 25 August 2005

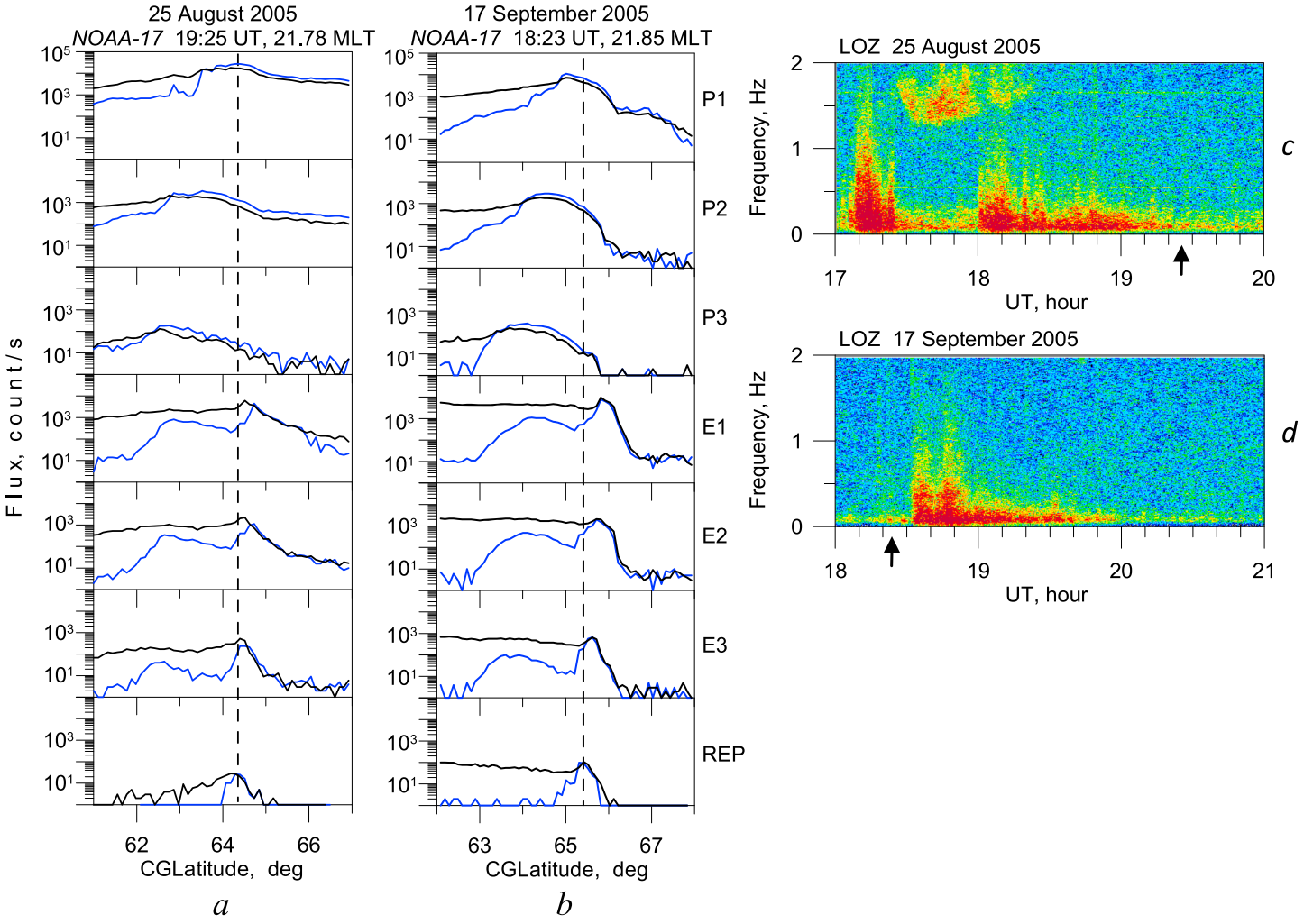

Figure 5. POES MEPED data and spectrograms for REP events of the *first* group on 25 August and 17 September 2005. (a and b, from top to bottom) Precipitating (blue line) and trapped (black line) flux of protons in channels P1, P2, and P3 and electrons in channels E1, E2, E3, and P6. The vertical dashed line indicates the maximal flux of precipitating relativistic electrons in the channel P6. (c and d) Spectrograms of geomagnetic pulsations from the ground station around the time of the REP events. The time of the REP observation is shown by the arrow.

coincides with the end of the interval of PiC pulsations. During both events ground magnetograms exhibit magnetic disturbances (not shown). In all, among 23 events of the *first* group, 18 events were associated with the noise or PiC pulsations, one event with PiB, and four events were not associated with any pulsations.

Figures 6a and 6b show the REP event of the *second* group observed on 10 November 2005 and the corresponding spectrogram. This REP event coincides with PiB pulsations. The REP event of 19 October 2005, also belonging to the second group, is observed during clear IPDP event (Figures 7a and 7b). In all, 32 events of the *second* group are related with PiC/noise, 11 events with PiB, 9 events do not associate with pulsations of any kind, and 11 events are observed during Pc1/IPDP.

Finally, Figure 8 shows three examples of REP events from the *third* group. The event of 21 August 2005 (Figure 8a) is observed during IPDP (Figure 8d), the event of 27 September 2005 (Figure 8b) correlates with quasi-monochromatic Pc1 pulsations (Figure 8e), and the event 13 July 2005 (Figure 8c) coincides with a burst of pulsations in the Pc1 range (Figure 8f). The latter event, which is the only morning side conjugated event of the *third* group shown in Figure 3 (bottom row), relates to strong magnetosphere compression (data not shown). Similarly, all other events of the *third* group demonstrate close connection with the EMIC wave signatures.

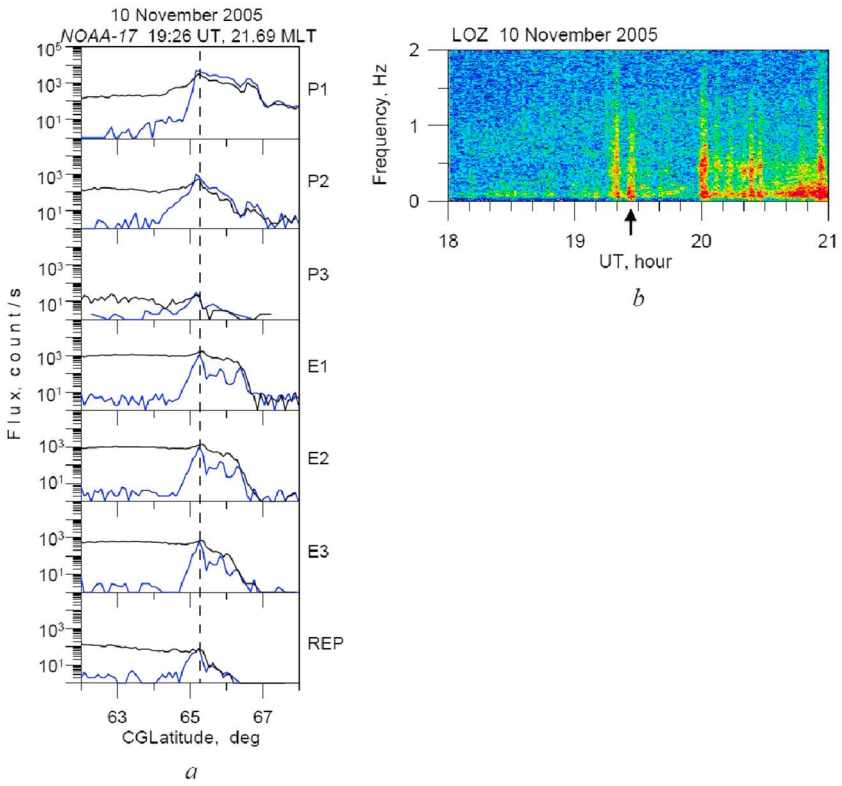

Figure 6. The same as in Figure 5 but for the REP event of the *second* group observed on 10 November 2005.

4. Discussion

The connection of all REP events of the *third* group with EMIC waves is not a surprise, because the definition of the *third* group contains enhancements of the proton flux within the anisotropy zone. Such proton bursts are believed to be the signature of EMIC waves. For example, *Yahnina et al.* [2003] correlated the proton bursts with Pc1 waves and found almost 100% correlation. Recently, *Hendry et al.* [2016] demonstrated that "EMIC wave-driven" REP events (that is, REP associated with proton enhancements [*Carson et al.*, 2013]) are closely associated with Pc1/IPDP signals.

More interestingly, 11 REP events of the *second* group are associated with Pc1 or IPDP. The events of the *second* group do not coincide with proton spikes; thus, they do not contain a clear indicator of the EMIC wave source on the REP field lines as the events of the *third* group do. Why are the Pc1 pulsations seen in these cases?

The possible reason might be related to the fact that sometimes it is difficult to distinguish between the events of the *second* and *third* groups. Let us consider the situation shown in Figure 7 where REP event is seen simultaneously with IPDP. In this case, the REP event at CGMLat = ~64.2 lies close to the equatorial edge of isotropic proton fluxes, just poleward of the isotropy boundary. Thus, this event can be assigned as the event of the *second* group. However, this isotropy boundary can be spurious while the real one can be located poleward. In such case, it is quite possible that there is a proton precipitation spike, which coincides with REP, but is within the anisotropy zone. It does not look as isolated because this spike is very close to the region of isotropic fluxes. If it is so, this event has to be assigned to the *third* group, and the REP event is the "EMIC wave-driven" one.

On the other hand, if the isotropy boundary seen in Figure 7 is real and divides the regions of adiabatic and nonadiabatic movement of protons, the REP event is within isotropic proton fluxes where EMIC waves cannot be generated (the electromagnetic ion cyclotron instability needs the transverse anisotropy of energetic protons). If so, the observed IPDP (Figure 7b) should have the source outside the REP location. In Figure 7, clear proton precipitating flux enhancement equatorward of the isotropy boundary is seen at CGMLat = ~63.3

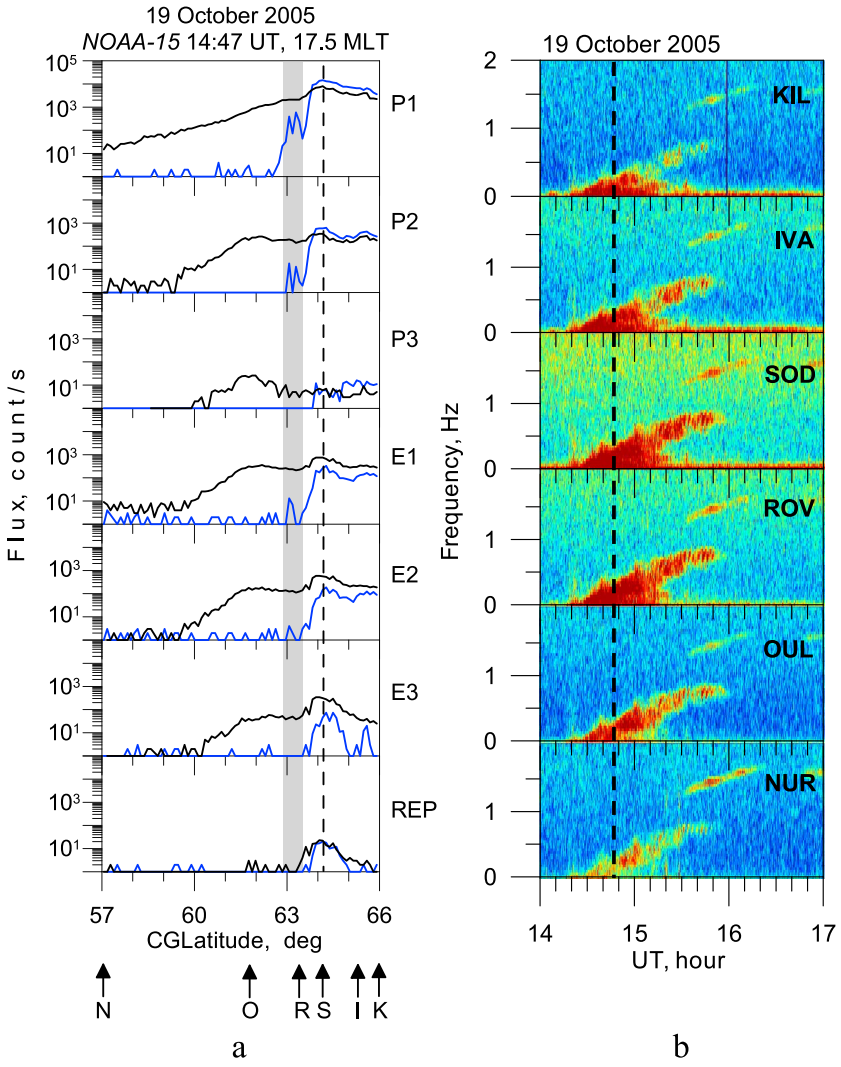

Figure 7. The same as in Figure 5 but for the REP event observed on 19 October 2005. Arrows on the bottom of the MEPED data mark (a) the locations of six stations of the Finnish network. Grey column in the MEPED data panel indicates location of the precipitating proton enhancement, that is, possible location of the EMIC wave source. (b) Spectrograms from all stations of the Finnish network are presented. Vertical dashed line on spectrograms shows the moment of the REP observation.

(indicated by grey column in Figure 7a). This proton flux enhancement is a good candidate for the IPDP source marker [*Yahnina et al.*, 2003; *Yahnin et al.*, 2009]. Such location of the EMIC wave source seems to be consistent with the distribution of the IPDP intensity along the Finnish chain of stations (Figure 7b). Indeed, the strongest amplitudes of the IPDP at the moment of the REP are observed at ROV and SOD, that is, possibly, equatorward of the REP location.

Thus, the consideration of the event in Figure 7 suggests two possible reasons for why the events of the second group can be associated with EMIC wave signatures. One is the erroneous assignment of the event to the *second* group. (Among 11 events, which we referred to the second group and which are observed simultaneously with EMIC wave signatures, we found five suspicious events that look like the event in Figure 7; that is, the REP is close to the vicinity of the equatorial edge of the isotropic fluxes region). Another reason is a simultaneous Pc1 wave source somewhere outside of the REP location [e.g., *Kim et al.*, 2011]. This possibility is clearly illustrated by the example in Figure 9. In this case, a REP was observed on 3 September 2005 by the NOAA 15 spacecraft at CGMLat = 65.73 close to the latitude of KIL (Figure 9b). Double-banded (~0.5 and ~1.2 Hz) Pc1 pulsations were detected by all ground stations during the event (Figure 9c). The strongest amplitudes of the pulsations were observed well equatorward of the REP

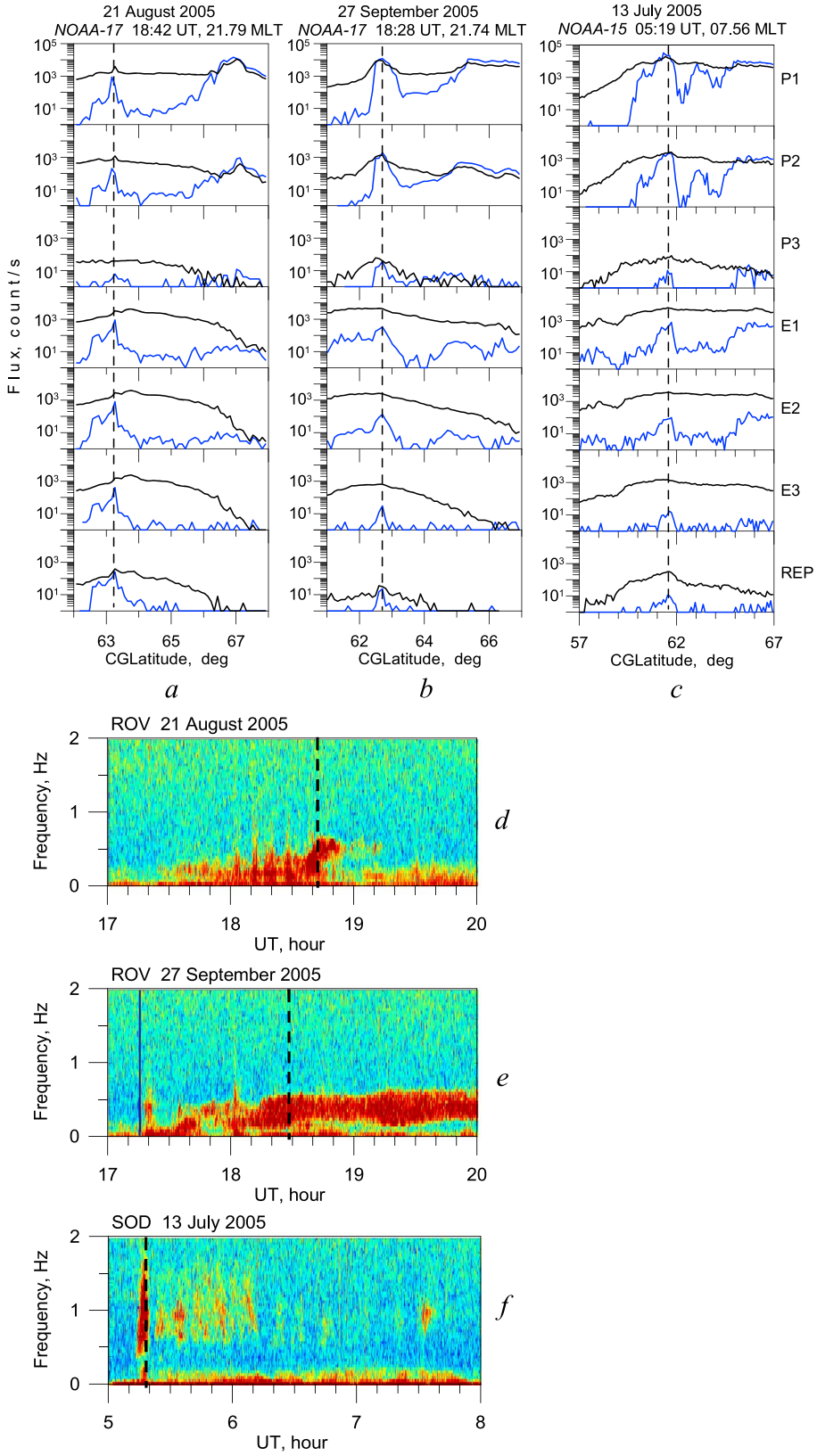

Figure 8. The same as in Figure 5 but for the REP events of the *third* group observed on (a and d) 21 August 2005, (b and e) 27 September 2005, (c and f) and 13 July 2005.

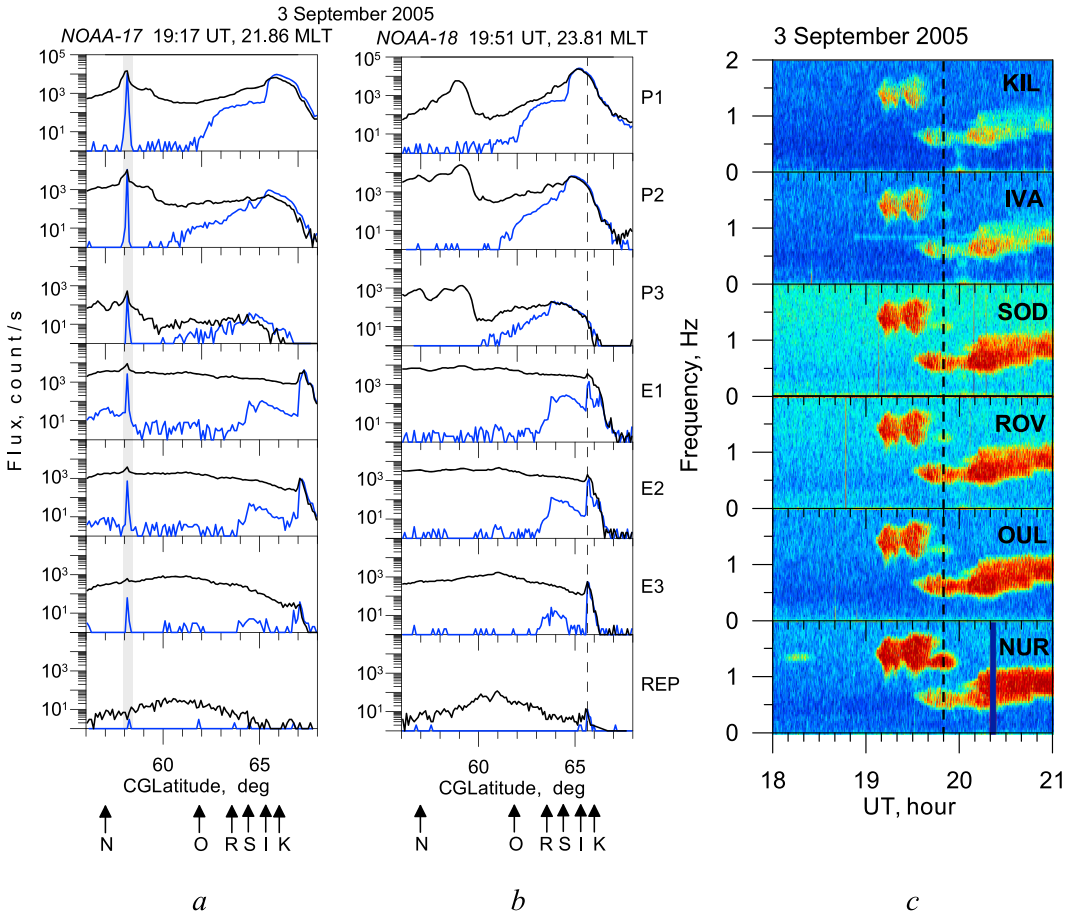

Figure 9. The same as in Figure 5 but for events of 3 September 2005. The MEPED data from two POES spacecraft (a) NOAA 17 and (b) NOAA 18 are shown. The REP event is marked by vertical dashed line in the data from NOAA 18. Grey column in the data from NOAA 17 marks the enhancement of precipitating protons that could be an indicator of the source of the Pc1 pulsations shown on (c) spectrograms of the Finnish network stations.

location. This suggests that the sources of EMIC waves are well outside of the source of REP. The particle signature of the EMIC wave source equatorward of the REP latitude (at CGMLat = 58) was indeed observed by the NOAA 17 spacecraft that flew in about 2 h of MLT eastward of the REP location. The proton burst seen in three upper panels of Figure 9a can be the particle counterpart of the Pc1 emission at 1.2 Hz, which is better seen in the southernmost station NUR. A particle indicator of the source of the 0.5 Hz emission is not found, but, in any case, the intensity of this emission is maximal below SOD and minimal in the REP location.

The majority of the REP events of the first and second groups are observed during the PiC/noise and PiB pulsations. The origin of these pulsations is, probably, the irregular fluctuations of the ionospheric and field-aligned currents due to enhanced auroral electron precipitation [e.g., *Engebretson et al.*, 1986; *Pashin et al.*, 1992; *Grant and Burns*, 1995], which indicates the development of geomagnetic activity (in particular, substorms).

During the enhanced geomagnetic activity, the configuration of the magnetic field in the near-Earth nightside magnetosphere becomes more stretched [e.g., *Lin and Barfield*, 1984]. Correspondingly, the region where the magnetic field curvature radius is small shifts to the Earth leading to the expansion of the region of nonadiabatic movement to the Earth and to the displacement of the isotropy boundary to lower latitudes [e.g., *Newell et al.*, 1998; *Lvova et al.*, 2005]. When approaching the Earth (lower latitudes) the region of the particle isotropization may overlap the outer radiation belt. In the region of overlapping, the movement of relativistic electrons becomes chaotic, and the electrons are scattered into the loss cone producing the REP events of the first group. This is consistent with fact that REP events of the *first* group coincide with the isotropy boundary of >0.8 MeV. According to calculations by *Bikkuzina et al.* [1998], the closest

location to the Earth of the electron isotropy boundary is in the midnight sector; outside this sector the distance of the isotropy boundary from the Earth dramatically increases. This is in accordance with the fact that REP events of the first group are observed only on the nightside. The near-Earth magnetic field becomes dipole like under quiet conditions, and the region of a small curvature radius retreats from the radiation belt into the region where the fluxes of relativistic electrons are negligible. This explains why almost all REP events of the first group are observed simultaneously with pulsations indicating enhanced geomagnetic activity.

Most REP events of the second group, which as we suppose are scattered by waves, are also associated with PiC/noise and PiB pulsations. This agrees with the fact that under disturbed magnetospheric conditions, the intensity of different wave modes, including those capable of scattering electrons into the loss cone (e.g., plasmaspheric hiss) and the probability of their observation, increases [e.g., *Meredith et al*., 2004, 2009; *Lam et al*., 2010; *Ma et al*., 2013; *Usanova et al*., 2012].

Hendry et al. [2016] correlated the "EMIC wave-driven REP" events (our events of the third group) with the ground observations of Pc1/IPDP pulsations and found good correlation for the REP events observed overhead the ground magnetometers. Our study confirms their conclusion. As it has already been noted, all REP events of the third group conjugated with ground magnetometers were observed during Pc1/IPDP in the range 0.1–2 Hz.

We would like to stress that although among 112 conjugated REP events, 37 events are observed during Pc1/IPDP pulsations; only 26 events of the third group undoubtedly coincide with the EMIC wave source and, therefore, can be the result of interaction of EMIC waves with radiation belt electrons (plus, possibly, no more than five events that we could erroneously refer to the second group). For the indubitable events of the second group, which are observed simultaneously with Pc1/IPDP, the EMIC wave source seems to be located outside the REP position. Thus, the proportion of the REP events, which are, possibly, produced by scattering by EMIC waves, can be estimated to be equal to some 23% (26 of 112 events). If all five suspicious events also belong to the third group, the percentage increases to 28%.

It is worth to note that the percentage of the REP events of the third group in subset of conjugated events is higher than that we found from in the whole data set used in this study (160 of 1057 events, that is, 15%). Perhaps, the difference is due to the small statistics of the conjugated events of this study. Anyway, this result shows that the EMIC wave driven REP events are not the prevailing fraction of all observed REP events.

5. Summary and Conclusion

Inspection of NOAA POES data for the interval from 1 July to 31 December 2005 revealed 1057 REP events. From this amount, 112 events were conjugated with the ground network of induction magnetometers measuring geomagnetic pulsations in the range of 0.1–5 Hz. Most REP events were associated with either no pulsations or pulsations PiB or PiC/noise. About one third of the conjugated REP events were accompanied by the EMIC wave signatures (geomagnetic pulsations in the Pc1 range), but only for a quarter of the events (23–28%) were spatially coincided with the signatures of the EMIC wave source.

Therefore, we conclude that interaction with EMIC waves is possibly important but not a prevailing mechanism to precipitate ~1 MeV relativistic electrons. Other mechanisms, including scattering in the region of small magnetic field line curvature radius and scattering by other waves, need more attention.

Acknowledgments
The authors thank NOAA for the access to the POES data (http://www.ngdc.noaa.gov/stp/satellite/poes/dataaccess.html). The efforts of SGO and PGI stuff providing the good quality data of the induction magnetometers are much appreciated. The list of REP events used in this study is available on request. This study was supported by the Academy of Finland (grant 294931).

References

Anderson, B. J., and D. C. Hamilton (1993), Electromagnetic ion cyclotron waves stimulated by modest magnetospheric compressions, *J. Geophys. Res.*, *98*, 11,369–11,382, doi:10.1029/93JA00605.

Anderson, B. J., R. E. Erlandson, and L. J. Zanetti (1992), A statistical study of Pc 1-2 magnetic pulsations in the equatorial magnetosphere: 1. Equatorial occurrence distributions, *J. Geophys. Res.*, *97*, 3075–3088, doi:10.1029/91JA02706.

Anderson, B. J., R. E. Erlandson, M. J. Engebretson, J. Alford, and R. L. Arnoldy (1996), Source region of 0.2 to 1.0 Hz geomagnetic pulsation bursts, *Geophys. Res. Lett.*, *23*, 769–772, doi:10.1029/96GL00659.

Bikkuzina G. R., V. A. Sergeev, and T. Bösinger (1998), Particle boundaries during a solar electron event, in *Polar Cap Boundary Phenomena*, *NATO ASI Book*, edited by J. Moen et al., pp. 355–367, Kluwer, Dordrecht.

Blum, L., X. Li, and M. Denton (2015), Rapid MeV electron precipitation as observed by SAMPEX/HILT during high-speed stream-driven storms, *J. Geophys. Res. Space Physics*, *120*, 3783–3794, doi:10.1002/2014JA020633.

Blum, L. W., Q. Schiller, X. Li, R. Millan, A. Halford, and L. Woodger (2013), New conjunctive CubeSat and balloon measurements to quantify rapid energetic electron precipitation, *Geophys. Res. Lett.*, *40*, 5833–5837, doi:10.1002/2013GL058546.

Bösinger, T., and A. G. Yahnin (1987), Pi1B type magnetic pulsation as a high time resolution monitor of substorm development, *Ann. Geophys.*, *5A*, 231–238.

Carson, B. R., C. J. Rodger, and M. A. Clilverd (2013), POES satellite observations of EMIC-wave driven relativistic electron precipitation during 1998–2010, *J. Geophys. Res. Space Physics*, *118*, 232–243, doi:10.1029/2012JA017998.
Chen, L., R. M. Thorne, and R. B. Horne (2009), Simulation of EMIC wave excitation in a model magnetosphere including structured high-density plumes, *J. Geophys. Res.*, *114*, A07221, doi:10.1029/2009JA014204.
Engebretson, M. J., L. J. Cahill Jr., J. D. Winningham, T. J. Rosenberg, R. L. Arnoldy, N. C. Maynard, M. Sugiura, and J. H. Doolittle (1986), Relations between morning sector Pi 1 pulsation activity and particle and field characteristics observed by the DE 2 satellite, *J. Geophys. Res.*, *91*, 1535–1547, doi:10.1029/JA091iA02p01535.
Evans, D. S., and M. S. Greer (2004), Polar orbiting environmental satellite space experiment monitor-2: Instrument descriptions and archive data documentation, NOAA Technical Memorandum version 1.3. NOAA Space Environment Center, Boulder, Colo.
Fukunishi, H., T. Toya, K. Koike, M. Kuwashima, and M. Kuwamura (1981), Classification of hydromagnetic emission based on frequency time spectra, *J. Geophys. Res.*, *86*, 9029–9039.
Grant, I. F., and G. B. Burns (1995), Observations and modeling of correlated Pi B magnetic and auroral luminosity pulsations, *J. Geophys. Res.*, *100*, 19,387–19,404, doi:10.1029/95JA00899.
Gustafsson, G., N. E. Papitashvili, and V. O. Papitashvili (1992), A revised corrected geomagnetic coordinate system for epochs 1985 and 1990, *J. Atmos. Terr. Phys.*, *54*, 1609–1631.
Halford, A. J., B. J. Fraser, and S. K. Morley (2010), EMIC wave activity during geomagnetic storm and nonstorm periods: CRRES results, *J. Geophys. Res.*, *115*, A12248, doi:10.1029/2010JA015716.
Hayakawa, M., S. Shimakura, T. Koboyashi, and N. Sato (1992), A study of polarisation of irregular pulsations of diminishing period and their generation mechanism, *Planet. Space Sci.*, *40*, 1081–1091.
Heacock, R. R. (1967), Two subtypes of type Pi micropulsations, *J. Geophys. Res.*, *72*, 3905–3917, doi:10.1029/JZ072i015p03905.
Hendry, A. T., C. J. Rodger, M. A. Clilverd, M. J. Engebretson, I. R. Mann, M. R. Lessard, T. Raita, and D. K. Milling (2016), Confirmation of EMIC wave-driven relativistic electron precipitation, *J. Geophys. Res. Space Physics*, *121*, 5366–5383, doi:10.1002/2015JA022224.
Imhof, W. L., H. D. Voss, J. B. Reagan, D. W. Datlowe, E. E. Gaines, and J. Mobilia (1986), Relativistic electron and energetic ion precipitation spikes near the plasmapause, *J. Geophys. Res.*, *91*, 3077–3088, doi:10.1029/JA091iA03p03077.
Imhof, W. L., H. D. Voss, J. Mobilia, D. W. Datlowe, and E. E. Gaines (1991), The precipitation of relativistic electrons near the trapping boundary, *J. Geophys. Res.*, *96*, 5619–5629, doi:10.1029/90JA02343.
Kangas, J., A. Guglielmi, and O. Pokhotelov (1998), Morphology and physics of short-period magnetic pulsations (a review), *Space Sci. Rev.*, *83*, 435–512.
Kim, H., M. R. Lessard, M. J. Engebretson, and M. A. Young (2011), Statistical study of Pc1–2 wave propagation characteristics in the high-latitude ionospheric waveguide, *J. Geophys. Res.*, *116*, A07227, doi:10.1029/2010JA016355.
Keika, K., K. Takahashi, A. Y. Ukhorskiy, and Y. Miyoshi (2013), Global characteristics of electromagnetic ion cyclotron waves: Occurrence rate and its storm dependence, *J. Geophys. Res. Space Physics*, *118*, 4135–4150, doi:10.1002/jgra.50385.
Lam, M. M., R. B. Horne, N. P. Meredith, S. A. Glauert, T. Moffat-Griffin, and J. C. Green (2010), Origin of energetic electron precipitation >30 keV into the atmosphere, *J. Geophys. Res.*, *115*, A00F08, doi:10.1029/2009JA014619.
Lin, C. S., and J. N. Barfield (1984), Magnetic field inclination angle at geosynchronous orbit, *Planet. Space Sci.*, *32*, 1283–1290.
Lvova, E. A., V. A. Sergeev, and G. R. Bagautdinova (2005), Statistical study of the proton isotropy boundary, *Ann. Geophys.*, *23*, 1311–1316, doi:10.5194/angeo-23-1311-2005.
Ma, Q., W. Li, R. M. Thorne, and V. Angelopoulos (2013), Global distribution of equatorial magnetosonic waves observed by THEMIS, *Geophys. Res. Lett.*, *40*, 1895–1901, doi:10.1002/grl.50434.
Meredith, N. P., R. B. Horne, R. M. Thorne, D. Summers, and R. R. Anderson (2004), Substorm dependence of plasmaspheric hiss, *J. Geophys. Res.*, *109*, A06209, doi:10.1029/2004JA010387.
Meredith, N. P., R. B. Horne, R. M. Thorne, and R. R. Anderson (2009), Survey of upper band chorus and ECH waves: Implications for the diffuse aurora, *J. Geophys. Res.*, *114*, A07218, doi:10.1029/2009JA014230.
Miyoshi, Y., K. Sakaguchi, K. Shiokawa, D. Evans, J. Albert, M. Connors, and V. Jordanova (2008), Precipitation of radiation belt electrons by EMIC waves, observed from ground and space, *Geophys. Res. Lett.*, *35*, L23101, doi:10.1029/2008GL035727.
Morley, S. K., S. T. Ables, M. D. Sciffer, and B. J. Fraser (2009), Multipoint observations of Pc1-2 waves in the afternoon sector, *J. Geophys. Res.*, *114*, A09205, doi:10.1029/2009JA014162.
Nakamura, R., D. N. Baker, J. B. Blake, S. Kanekal, B. Klecker, and D. Hovestadt (1995), Relativistic electron precipitation enhancements near the outer edge of the radiation belt, *J. Geophys. Res.*, *22*, 1129–1132, doi:10.1029/95GL00378.
Nakamura, R., M. Isowa, Y. Kamide, D. N. Baker, J. B. Blake, and M. Looper (2000), SAMPEX observations of precipitation bursts in the outer radiation belt, *J. Geophys. Res.*, *105*, 15,875–15,886, doi:10.1029/2000JA900018.
Newell, P. T., V. A. Sergeev, G. R. Bikkuzina, and S. Wing (1998), Characterizing the state of the magnetosphere: Testing the ion precipitation maxima latitude (b2i) and the ion isotropy boundary, *J. Geophys. Res.*, *103*, 4739–4745, doi:10.1029/97JA03622.
Pashin, A. B., V. R. Tagirov, T. Bosinger, A. G. Yahnin, and S. A. Chernouss (1992), A study of variations of the aurora intensity and irregular magnetic pulsations during breakup [in Russian], *Magnetos. Res.*, *18*, 66–70.
Pikkarainen, T., J. Kangas, B. Kiselev, N. Maltseva, R. Rakhmatulin, and S. Solovjev (1983), Type IPDP magnetic pulsations and the development of their sources, *J. Geophys. Res.*, *88*(A8), 6204–6212, doi:10.1029/JA088iA08p06204.
Rodger, C. J., M. A. Clilverd, J. C. Green, and M. M. Lam (2010a), Use of POES SEM-2 observations to examine radiation belt dynamics and energetic electron precipitation into the atmosphere, *J. Geophys. Res.*, *115*, A04202, doi:10.1029/2008JA014023.
Rodger, C. J., B. R. Carson, S. A. Cummer, R. J. Gamble, M. A. Clilverd, J. C. Green, J.-A. Sauvaud, M. Parrot, and J.-J. Berthelier (2010b), Contrasting the efficiency of radiation belt losses caused by ducted and nonducted whistler mode waves from ground-based transmitters, *J. Geophys. Res.*, *115*, A12208, doi:10.1029/2010JA015880.
Rodger, C. J., A. T. Hendry, M. A. Clilverd, C. A. Kletzing, J. B. Brundell, and G. D. Reeves (2015), High-resolution in situ observations of electron precipitation causing EMIC waves, *Geophys. Res. Lett.*, *42*, 9633–9641, doi:10.1002/2015GL066581.
Sakaguchi, K., K. Shiokawa, A. Ieda, Y. Miyoshi, Y. Otsuka, T. Ogawa, M. Connors, E. F. Donovan, and F. J. Rich (2007), Simultaneous ground and satellite observations of an isolated proton arc at subauroral latitudes, *J. Geophys. Res.*, *112*, A04202, doi:10.1029/2006JA012135.
Sandanger, M., F. Søraas, K. Aarsnes, K. Oksavik, and D. S. Evans (2007), Loss of relativistic electrons: Evidence for pitch angle scattering by electromagnetic ion cyclotron waves excited by unstable ring current protons, *J. Geophys. Res.*, *112*, A12213, doi:10.1029/2006JA012138.
Sergeev, V. A., and N. A. Tsyganenko (1982), Energetic particle losses and trapping boundaries as deduced from calculations with a realistic magnetic field model, *Planet. Space Sci.*, *30*, 999–1006, doi:10.1016/0032-0633(82)90149-0.
Shklyar, D. R., and B. Kliem (2006), Relativistic electron scattering by electrostatic upper hybrid waves in the radiation belt, *J. Geophys. Res.*, *111*, A06204, doi:10.1029/2005JA011345.

Smith, D. M., E. P. Casavant, M. D. Comess, X. Liang, G. S. Bowers, R. S. Selesnick, L. B. N. Clausen, R. M. Millan, and J. G. Sample (2016), The causes of the hardest electron precipitation events seen with SAMPEX, *J. Geophys. Res. Space Physics*, *121*, 8600–8613, doi:10.1002/2016JA022346.

Summers, D., B. Ni, and N. P. Meredith (2007), Timescales for radiation belt electron acceleration and loss due to resonant wave-particle interactions: 2. Evaluation for VLF chorus, ELF hiss, and electromagnetic ion cyclotron waves, *J. Geophys. Res.*, *112*, A04207, doi:10.1029/2006JA011993.

Thorne, R. M., and C. F. Kennel (1971), Relativistic electron precipitation during magnetic storm main phase, *J. Geophys. Res.*, *76*, 4446–4453, doi:10.1029/JA076i019p04446.

Troitskaya, V. A. (1961), Pulsations of the Earth's electromagnetic field with periods of 1 to 15 seconds and their connection with phenomena in high atmosphere, *J. Geophys. Res.*, *66*, 5–18, doi:10.1029/JZ066i001p00005.

Usanova, M. E., I. R. Mann, J. Bortnik, L. Shao, and V. Angelopoulos (2012), THEMIS observations of electromagnetic ion cyclotron wave occurrence: Dependence on *AE*, *SYM-H*, and solar wind dynamic pressure, *J. Geophys. Res.*, *117*, A10218, doi:10.1029/2012JA018049.

Yahnin, A. G., and T. A. Yahnina (2007), Energetic proton precipitation related to ion-cyclotron waves, *J. Atmos. Sol. Terr. Phys.*, *69*(14), 1690–1706, doi:10.1016/j.jastp.2007.02.010.

Yahnin, A. G., T. A. Yahnina, and H. U. Frey (2007), Subauroral proton spots visualize the Pc1 source, *J. Geophys. Res.*, *112*, A10223, doi:10.1029/2007JA012501.

Yahnin, A. G., T. A. Yahnina, H. U. Frey, T. Bösinger, and J. Manninen (2009), Proton aurora related to intervals of pulsations of diminishing periods, *J. Geophys. Res.*, *114*, A12215, doi:10.1029/2009JA014670.

Yahnin, A. G., T. A. Yahnina, N. V. Semenova, B. B. Gvozdevsky, and A. B. Pashin (2016), Relativistic electron precipitation as seen by NOAA POES, *J. Geophys. Res. Space Physics*, *121*, 8286–8299, doi:10.1002/2016JA022765.

Yahnina, T. A., A. G. Yahnin, J. Kangas, J. Manninen, D. S. Evans, A. G. Demekhov, V. Y. Trakhtengerts, M. F. Thomsen, G. D. Reeves, and B. B. Gvozdevsky (2003), Energetic particle counterparts for geomagnetic pulsations of Pc1 and IPDP types, *Ann. Geophys.*, *21*, 2281–2292.

Yahnina, T. A., H. U. Frey, T. Bösinger, and A. G. Yahnin (2008), Evidence for subauroral proton flashes on the dayside as the result of the ion cyclotron interaction, *J. Geophys. Res.*, *113*, A07209, doi:10.1029/2008JA013099.

Yando, K., R. M. Millan, J. C. Green, and D. S. Evans (2011), A Monte Carlo simulation of the NOAA POES medium energy proton and electron detector instrument, *J. Geophys. Res.*, *116*, A10231, doi:10.1029/2011JA016671.

Zhang, Y., L. J. Paxton, and Y. Zheng (2008), Interplanetary shock induced ring current auroras, *J. Geophys. Res.*, *113*, A01212, doi:10.1029/2007JA012554.